# Impact of N-Truncated A$\beta$ Peptides on Cu- and Cu(A$\beta$)-Generated ROS: Cu I Matters!

Charlène Esmieu, Guillaume Ferrand, Valentina Borghesani, Christelle Hureau

▶ **To cite this version:**

Charlène Esmieu, Guillaume Ferrand, Valentina Borghesani, Christelle Hureau. Impact of N-Truncated A$\beta$ Peptides on Cu- and Cu(A$\beta$)-Generated ROS: Cu I Matters!. Chemistry - A European Journal, 2021, 27 (5), pp.1777-1786. 10.1002/chem.202003949 . hal-03383515

**HAL Id: hal-03383515**
**https://hal.science/hal-03383515**

Submitted on 18 Oct 2021

**HAL** is a multi-disciplinary open access archive for the deposit and dissemination of scientific research documents, whether they are published or not. The documents may come from teaching and research institutions in France or abroad, or from public or private research centers.

L'archive ouverte pluridisciplinaire **HAL**, est destinée au dépôt et à la diffusion de documents scientifiques de niveau recherche, publiés ou non, émanant des établissements d'enseignement et de recherche français ou étrangers, des laboratoires publics ou privés.

# Impact of N-Truncated Aβ Peptides on Cu- and Cu(Aβ)-Generated ROS: Cu(I) Matters!

C. Esmieu,*[a] G. Ferrand,[a, b] V. Borghesani,[a, b] ≠ and C. Hureau*[a, b]

**Abstract:**

The *in vitro* Cu($Aβ_{1-x}$) induced ROS production has been extensively and thoroughly studied. Conversely, the ability of N-truncated isoforms of Aβ to alter the Cu-induced ROS production has been overlooked even though they are main constituents of amyloid plaques found in the human brain. N-truncated peptides at the positions 4 and 11 ($Aβ_{4-x}$ and $Aβ_{11-x}$) contain an amino-terminal copper and nickel (ATCUN) binding motif ($NH_2$-Xxx-Zzz-His) that confer them different coordination sites and higher affinities for Cu(II) compared to the Aβ peptide. It has further been proposed that the role of $Aβ_{4-x}$ peptide is to quench Cu(II) toxicity in the brain. However, the role of Cu(I) coordination has never been investigated so far. In contrast to Cu(II), the Cu(I) coordination is expected to be the same for N-truncated and N-intact peptides. Here, we report in-depth spectroscopic characterizations (Cu(II) and Cu(I)) complexes of the $Aβ_{4-16}$ and $Aβ_{11-16}$ N-truncated peptides and ROS production studies with copper (Cu(II) and Cu(I)) complexes of the $Aβ_{4-16}$ and $Aβ_{11-16}$ N-truncated peptides. Our findings show that the N-truncated peptides do produce ROS when Cu(I) in present in the medium, although to a lesser extent than the unmodified counterpart. In addition, when used as competitor ligands (*id est*, in the presence of $Aβ_{1-16}$), the N-truncated peptides are not able to fully preclude Cu($Aβ_{1-16}$) induced ROS production.

## Introduction

Alzheimer disease (AD) is the most common cause of dementia, affecting more than 30 million people in the world, characterized by a brain deterioration leading to difficulties with memory, behaviour, and thinking. According to the "amyloid cascade hypothesis" an abnormal amyloid deposits formation composed of amyloid-β peptides (Aβ) occurs in AD brain in extracellular locations at the early stage of the disorder.[1] Aggregation of Aβ is linked to an accumulation of the peptide induced by an imbalance between its clearance and its production. Aβ is a fragment of 40-42 amino acids derived from the proteolytic cleavage of the amyloid precursor protein (APP) by the β- and γ-secretases. Studies of the composition of the senile plaques in the middle of the eighty's showed a heterogeneity of Aβ sequences including the presence of the N-truncated isoform at position 4 ($Aβ_{4-x}$).[2] Since then, numerous studies have shown the presence of a large number of N-terminally altered isoforms as the $Aβ_{3-x}$ and $Aβ_{11-x}$.[3] N-truncated Aβs are produced either from the proteolysis of the full length ($Aβ_{1-x}$), or by dedicated proteases that process directly the APP.[4] According to ref. 5, isolated plaques from sporadic AD people contain up to 18,6 % of $Aβ_{11-42}$, a level comparable to the $Aβ_{1-42}$ isoform.[5] $Aβ_{11-42}$ exposes a glutamic acid residue, which allows the N-terminal cyclization of the peptide to its pyroglutamate derivative ($pEAβ_{11-42}$). It has been proposed that $pEAβ_{11-42}$ also forms slowly over time.[6] Both forms are found in the senile plaques and cerebrospinal fluid. Recently, the N-truncated isoforms have drawn much more attention due to their putative protective role against ROS.[3b, 7]

The Aβ full length ($Aβ_{1-x}$) possesses two main domains, while the last amino acid are involved in aggregation processes, the first fourteenth are responsible of the coordination of metal ions, mainly copper and zinc.[3d, 8] Cu ion bound to Aβ is able to catalyse the production of reactive oxygen species (ROS) through successive stepwise reduction of dioxygen.[9] This ROS production is assumed to be part of the enhancement of the oxidative stress found in AD brain that drives the disease.[10] The copper coordination to the Aβ or its validated model $Aβ_{1-16}$ (sequence in Scheme 1) has been widely investigated.[10-11] The coordination sites of Cu(I) and Cu(II) to Aβ near physiological pH are depicted in Scheme 1.[8] Within $Aβ_{1-16}$ the Cu(II) is coordinated by the N-terminal amine, the adjacent carbonyl group from the peptide backbone, and two imidazole rings from two among the three Histidine (His) side-chain in a square-planar geometry with an apparent affinity constant of $10^{10}$ $M^{-1}$ at pH 7.4.[12] The N-terminal truncation of Aβ at position 4 and 11 releases a peptide containing an amino-terminal copper and nickel motif (ATCUN, $NH_2$-Xxx-Zzz-His) which is known to bind Cu(II) with high affinity constant (~$10^{14}$ $M^{-1}$).[13] The binding site of $Aβ_{4/11-16}$ (sequence in Scheme 1) is constituted by the N-terminal amine, the proximal (δ) nitrogen atom of the His side chain and both deprotonated amides of the peptide backbone in between the N-terminal amine and the His (Scheme 1).[13-14]

In contrast, the Cu(I) coordination site is expected to be similar for the three peptides ($Aβ_{1/4/11-16}$) since the two imidazole rings required for Cu(I) binding are present in the three sequences. It is thus anticipated that Cu(I) lies in a digonal environment made by two imidazole groups from the His residues at position 6, 13 and 14 (13 and 14 only for the $Aβ_{11-16}$).[15] The affinity is also expected to be similar between the three peptides, while the values reported for $Aβ_{1-16}$ range between $10^7$ to $10^{10}$ $M^{-1}$.[15a, 16]

A vast amount of *in vitro* investigations on the production of ROS by the full length $Aβ_{1-40/42}$ or its C-terminally truncated model $Aβ_{1-16}$ in presence of Cu ions have been performed.[9] Importantly it was evidenced by electrochemistry that the direct electron transfer between $Cu^{I}(Aβ_{1-16})$ and $Cu^{II}(Aβ_{1-16})$ is hampered by a

[a] Dr. C. Esmieu, G. Ferrand, Dr. V. Borghesani, Dr C. Hureau
CNRS, LCC (Laboratoire de Chimie de Coordination)
205 route de Narbonne,BP 44099 31077 Toulouse Cedex 4, France
E-mail : christelle.hureau@lcc-toulouse.fr and charlene.esmieu@lcc-toulouse.fr
[b] G. Ferrand, Dr. V. Borghesani and Dr. C. Hureau
University of Toulouse, UPS, INPT
31077 Toulouse Cedex 4, France
≠ Dr. V. Borghesani current address School of Chemistry, University of Birmingham, Edgbaston, B15 2TT, UK

Supporting information for this article is given *via* a link at the end of

large reorganization energy and thus proceeds *via* an unusual mechanism.[9a] ROS are therefore produced by an "in between" state (IBS) in equilibrium with the $Cu^{I}(A\beta_{1-16})$ and $Cu^{II}(A\beta_{1-16})$. Structurally, it has been proposed that the Cu in the IBS is linked to the N-terminal amine, the carboxylate group from Asp1, and one imidazole group from one His of the peptide,[9e, 17] but this model is still under discussion.[18]

Conversely, researches on the ability of N-terminally truncated $Cu(A\beta_{4-16})$ to produce ROS are only very recent (and limited to studies with Cu(II) only).[7a, 13a, 19] It has been shown that the $A\beta_{4-16}$ presents a highly ordered metal binding site of low redox activity in presence of Cu(II) and ascorbate.[13a] Additionally it has been suggested that it can extract Cu(II) from $Cu^{II}(A\beta_{1-16})$ and could have a crucial role in metal homeostasis [7a, 20] and thus could be beneficial in the context of AD as an intrinsic competitor to prevent the ROS production generated by the Cu-metallated $A\beta_{1-x}$.[7a, 7c]

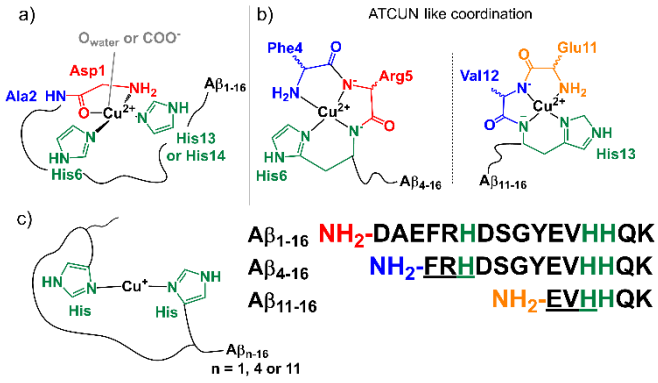


*Scheme 1 : Representation of the main coordination site of Cu(II) bound to (a) $A\beta_{1-16}$, (b) $A\beta_{4-16}$ and $A\beta_{11-16}$, (c) shared Cu(I) coordination site at physiological pH and sequence of the Aβ peptides under investigation in the paper with the His in green and the ATCUN motif underlined*

To gain a better understanding of the coordination chemistry of N-truncated peptides containing a ATCUN motif involved in AD, we have investigated the Cu(II) and Cu(I) binding properties of the $A\beta_{4-16}$ and $A\beta_{11-16}$ isoforms, and compared them to the $A\beta_{1-16}$. Furthermore, we have challenged the ROS production ability of these two $Cu(A\beta_{4/11-16})$ in a more biologically relevant medium containing Cu(I). Finally, we further studied the ability of the N-truncated isoforms $A\beta_{4/11-16}$ to extract Cu(I) and Cu(II) from the $A\beta_{1-16}$ peptide and to impact the ROS production by $Cu(A\beta_{1-16})$. We confirm that $A\beta_{4-16}$ and $A\beta_{11-16}$ are both able to form redox inert Cu(II) complexes and can extract Cu(II) from $Cu(A\beta_{1-16})$. However and more importantly, we demonstrate that the high-affinity and redox-inert Cu(II) ATCUN binding site of the N-truncated peptides is not enough to preclude ROS production. We show that this is due to (1) the capability of the peptides to bind Cu(I) and (2) kinetically competitive processes (formation of the ATCUN Cu(II) site versus reduction of Cu(II)-bound to $A\beta_{4/11-16}$ in another site than the ATCUN one). In addition, when $A\beta_{4/11-16}$ are regarded as intrinsic redox-silencing chelators, their effect on ROS production is dependent on the starting conditions, and again when Cu(I) is present in the medium, ROS production is only moderately lessen, in line with similar Cu(I) affinity of the N-truncated peptides versus the unmodified counterpart. As a result, a biologically relevant mixture of the various Cu(peptides) species can produce ROS in presence of Cu(I), dioxygen and ascorbate, which mirror physiological conditions.

## Results and Discussion

### Characterization of $Cu(A\beta_{4-16})$ and $Cu(A\beta_{11-16})$

**Cu(II) binding kinetics**. Stopped flow measurements have been realized in order to qualitatively evaluate the kinetics of Cu(II) coordination by the two N-truncated peptides (Figure S1). The stopped-flow system used is coupled to diode array detector in the 250-720 nm range allowing to monitor of the d-d band increase (for the $Cu^{II}(A\beta_{4/11-16})_{ATCUN}$ complexes, $\lambda_{max}$ = 520 nm), linked to the formation of the Cu(II) complexes, over time. In a quasi-stoichiometric amount of Cu(II) (0.9 equiv. per peptide) and at about 0.5 mM, $A\beta_{11-16}$ is faster in coordinating Cu(II) than $A\beta_{4-16}$, with $t_{1/2}$ = 0.13 ± 0.02 s *vs* $t_{1/2}$ = 0.45 ± 0.1 s for $A\beta_{11-16}$ and $A\beta_{4-16}$, respectively. The value found for the $A\beta_{4-16}$ agrees fairly well with that recently determined by competition and double mixing stopped flow experiments and attributed the formation of the $Cu^{II}(A\beta_{4-16})_{ATCUN}$ motif once the Cu(II) is anchored to the peptide.[21] Additionally, the value found for $Cu^{II}(A\beta_{11-16})$ is in accordance with the value very recently determined in ref.[22] on the short GGH peptide by classical stopped flow experiments and attributed to the reshuffling of the Cu(II) site forming the ATCUN motif after initial anchoring to the N-terminal and side-chain of His groups. In addition, it was not possible to measure the rate of Cu(II) binding to the $A\beta_{1-16}$ under the very same conditions, thus indicating that Cu(II) anchoring to the peptide (mainly *via* His or carboxylate containing amino-acid residues),[11c] is much faster (Figure S1). This confirms that the rate determined with the $A\beta_{11-16}$ and $A\beta_{4-16}$ mainly witnesses the formation of the ATCUN site around the Cu(II) ion.

The difference observed between the two peptides (formation of $Cu^{II}(A\beta_{4-16})_{ATCUN}$ about three times slower than that of $Cu^{II}(A\beta_{11-16})_{ATCUN}$) may be linked to the presence of the His13 and His14. Such His dyad creates a second independent and thus competing site in $A\beta_{4-16}$ as recently observed for similar peptides encompassing both a ATCUN and a His dyad site.[23] Conversely, the His dyad belongs to the ATCUN motif in $A\beta_{11-16}$ thus helping the anchoring of Cu(II) near the final ATCUN site.

Briefly, the values we determined here mainly mirror the time required to accommodate the Cu(II) in the ATCUN site, in line with a very fast anchoring process (thus not rate-limiting) at such high concentration.

**Electron Paramagnetic Resonance.** Both complexes $Cu^{II}(A\beta_{4-16})$ and $Cu^{II}(A\beta_{11-16})$ display a classical EPR signal for a 4N coordination, with superhyperfine lines in the perpendicular region indicative of N equatorial ligands (Figure S2 (b) and (d)) and reminiscent of Cu(II) bound in a ATCUN[7b, 24] motif including those obtained with $A\beta_{11-15}$ and $A\beta_{4-16}$.[13-14, 25] This signature strongly differs from the one of $Cu^{II}(A\beta_{1-16})$ (Figure S2 (a)) allowing to easily monitor the removing of Cu(II) from $Cu^{II}(A\beta_{1-16})$ by the two N-truncated peptides. EPR signatures were identical with or without $A\beta_{1-16}$ demonstrating that the final species formed in the presence of an equimolar mixture of $A\beta_{4/11-16}$ and $A\beta_{1-16}$ is the $Cu^{II}(A\beta_{4/11-16})_{ATCUN}$ complex (Figure S2 (c) and (e)). The EPR parameters are summarized in Table 1.

**Electrochemistry.** The cyclic voltammograms (CV) of Cu bound to $Cu^{II}(A\beta_{4-16})$ and $Cu^{II}(A\beta_{11-16})$ are shown in Figure 1 and Figure S3.

The $A\beta_{4-16}$ peptide alone displays an irreversible oxidation at $E^{pa}$ = 0.76 V *vs* SCE (1.00 V vs NHE) corresponding to the Tyr10 oxidation (Figure S3).[13a, 26] The $Cu^{II}(A\beta_{4-16})$ complex shows an irreversible anodic process at $E^{pa}$ = 0.81 V *vs* SCE (1.05 V *vs* NHE). This potential is close to the early reported value for the oxidation of Cu(II) to Cu(III) in an ATCUN motif.[13a, 27] The unusual intensity of this peak originated from the addition of the two processes mentioned before (*i. e.* Tyr10 and Cu(II) to Cu(III) oxidations). The $Cu^{II}(A\beta_{4-16})$ complex is reduced at $E^{pc}$ = −1.06 V *vs* SCE (-1.30 V vs NHE), leading to $Cu^{I}(A\beta_{4-16})^{*}$ species that chemically evolves toward the stable $Cu^{I}(A\beta_{4-16})_{L}$ species that is reoxidized at $E^{pa}$ = 0.24 V *vs* SCE (0.48 V vs NHE). It can be postulated that the Cu(II) coordination changes upon reduction from a typical 4N coordination by the ATCUN motif to a linear coordination between to imidazole rings of the His residues to accommodate the Cu(I) ion. The electrochemical pattern is indeed strongly reminiscent of the oxidation of a His-Cu(I)-His species.[28]

The $A\beta_{11-16}$ peptide alone yield no electrochemical activity in line with the absence of redox active amino-acid residue (*i.e.*Tyr10) in the peptide sequence (Figure S3). As for the $Cu^{II}(A\beta_{4-16})$, the $Cu^{II}(A\beta_{11-16})$ can be oxidized to $Cu^{III}(A\beta_{11-16})$ at $E^{pa}$ = 0.78 V *vs* SCE (1.02 V vs NHE) but this time the $Cu^{III}$ species can be reduced at $E^{pa}$ = 0.67 V *vs* SCE (0.91 V vs NHE) leading to a quasi-reversible process. The reversibility of the Cu(III/II) process in the ATCUN motif is dependent on the nature of the Xxx and Zzz amino acid residues which can explain the difference with $Cu^{II}(A\beta_{4-16})$ in addition to the absence of the concomitant oxidation of Tyr10.[7b, 29] $Cu^{II}(A\beta_{11-16})$ shows an irreversible cathodic peak at $E^{pc}$ = −1.26 V *vs* SCE (-1.50 V vs NHE) attributed to its reduction to a $Cu^{I}(A\beta_{11-16})$* complex followed by a structural rearrangement leading to a re-oxidation peak at $E^{pa}$ = 0.27 V *vs* SCE (0.51 V *vs* NHE), as observed for $Cu^{II}(A\beta_{4-16})$. The different cathodic potentials between the two complexes can tentatively be attributed to (i) a less stabilized ATCUN motif in the $Cu^{II}(A\beta_{4-16})$ due to the presence of Arg5 adjacent to His6. Such proximity between these two amino-acid residues has been previously proposed to hinder the Cu(II) binding by His[30] and (ii) more stable Cu(I) species due to the presence of three His leading to three possible His binding dyads. Conversely, the re-oxidation peak of the electrochemically generated Cu(I) species are at the same potential value in line with similar Cu(I) coordination. To summarize, we have thus observed a classical ECEC (Electrochimical-Chemical-Electrochemical-Chemical)
mechanism, where the first electrochemical process is the reduction of the Cu(II) in the ATCUN site, the first chemical evolution leads to a linearly bound bis-His Cu(I) species, that is oxidized (second electrochemical process) and evolves back to the initial Cu(II) species.

For both N-truncated sequences the Cu(II) complexes can be reduced to Cu(I) but at a very low potential, $E^{pc}$ < -1 V *vs* SCE. This reduction potential of the Cu(II) complexes is well beyond the oxidation potential of ascorbate, hence, the Cu(II) complexes are expected to be stable upon reduction with ascorbate.[31] Electrochemical potential (EP) are summarized in Table 1.

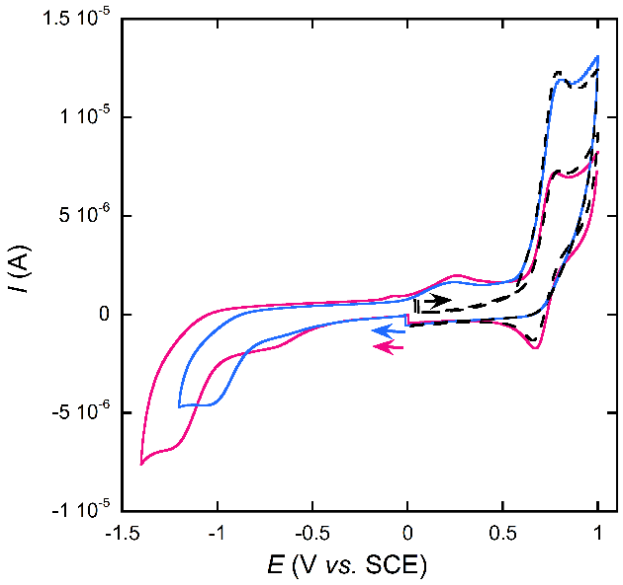


Figure 1 : Cyclic voltammogram (CV) of $Cu^{II}(A\beta_{11-16})$ (pink line) and $Cu^{II}(A\beta_{4-16})$ (blue line). The dotted black lines are CV measured in oxidation showing no electrochemical process at 0.24 V *vs* SCE. [$A\beta_{4/11-16}$] = 0.2 mM, [Cu(II)] = 0.19 mM in [phosphate buffer] = 50 mM at pH 7.4 under argon. Scan rate = 100 $mV.s^{-1}$; WE = Glassy carbon, Ref = SCE, CE = Pt wire. First scans are shown starting from the open circuit potential (from the arrows).

**Cu(I) NMR.** NMR experiments were performed to evaluate the Cu(I) binding to the different peptides. Expected chemical shift of the protons in the Cu(I) vicinity are observed for $Cu^{I}(A\beta_{1-16})$ complex. For instance, in the aromatic region the $H_{\delta}$ and $H\varepsilon$ protons of His, present at around 7.70 and 6.85 ppm, are strongly shifted indicating that the His residue are involved in Cu(I) binding (Figure 2a).[9b] Similar trends are followed by the two N-truncated peptides, with a large shift of the protons of the His residues. Interestingly the protons of the Val12 are strongly shifted for the $A\beta_{11-16}$ peptide but are not really affected in the $A\beta_{1-16}$ and $A\beta_{4-16}$ cases. This is strongly indicative that the coordination of Cu(I) into the $A\beta_{11-16}$ is different than the one in $A\beta_{1-16}$ and $A\beta_{4-16}$. From a peptide sequence point of view, $A\beta_{11-16}$ lacks the His6, implying that the Cu(I) is coordinated only by the His 13 and His 14. The different proton behavior of Val12 observed for $A\beta_{11-16}$ suggests the involvement of the His6 in the Cu(I) coordination with the $A\beta_{1-16}$ and $A\beta_{4-16}$ peptides in contrast to our previous report.[9b] The present observation is consistent with a recently published article showing that His6 is the His mainly involved in Cu(I) binding.[15a]

Table 1: Apparent binding affinities determined for Cu(I), conditional binding affinities reported for Cu(II), redox potentials, UV-vis and EPR parameters determined for $^{65}$Cu(II) for Aβ$_{4-16}$ and Aβ$_{11-16}$ peptides.

| *Peptide* | *[a]Ka ($\mu$M$^{-1}$) pCu for Cu(I)[a]* | *[c]Ka (M$^{-1}$) pCu for Cu(II)[a]* | *EP (vs NHE)* | | | *UV-Vis* | *EPR (A in G)[b]* | | |
|---|---|---|---|---|---|---|---|---|---|
| | | | *$Cu^{2+}\rightarrow Cu^{+}$* | *$Cu^{+}\rightarrow Cu^{2+}$* | *$Cu^{2+}\rightarrow Cu^{3+}$* | *$\lambda_{max}$ (nm)* (ε in M$^{-1}$.cm$^{-1}$) | $g_{\perp}$ | $g_{\parallel}$ | $A_{\parallel}$ |
| Aβ$_{4-16}$ | 3.7 ± 0.4<br>*5.9* | *~10$^{13}$*<br>*12.8 [13a]* | -1.30 V | 0.48 V | 1.05 V | 520 (100) | 2.055 | 2.18 | 211 |
| Aβ$_{11-16}$ | 1.9 ± 0.5<br>*5.6* | *~10$^{13}$*<br>*12.8 [13b]* | -1.50 V | 0.51 V | 1.02 V | 522 (102) | 2.049 | 2.19 | 217 |
| Aβ$_{1-16}$ | 7.5 ± 1.0<br>*6.2* | *~10$^{10}$*<br>*8.9 [12a]* | | | | 625 (65) | 2.06 | 2.27 | 181 |

[a]pCu = -log [Cu]$_{free}$ for 1.2 *[Cu] = [L] and [Cu] = 10 µM. [b]EPR parameters were determined in 50 mM HEPES, pH 7.4 buffer containing 10% glycerol (v/v).

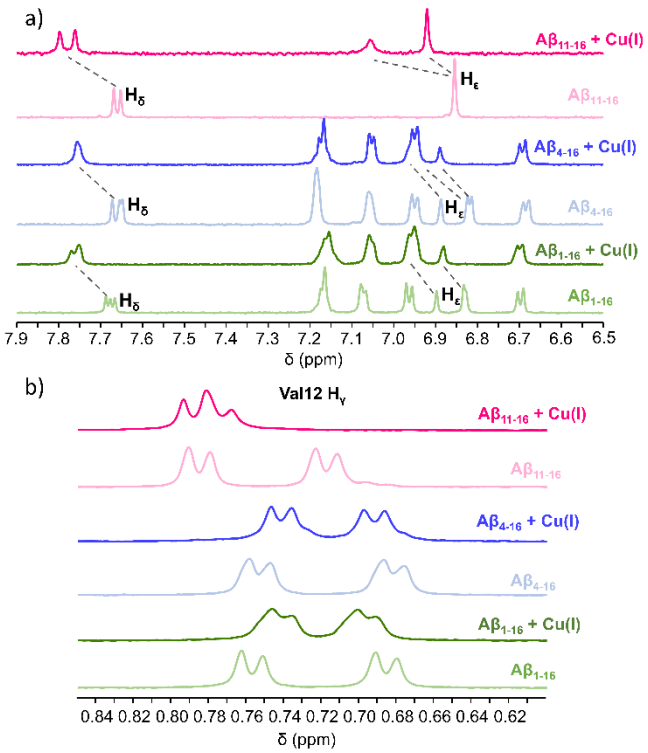


Figure 2 : $^{1}$H NMR spectra of Aβ$_{1-16}$ (light green) with 1 equivalent of Cu(I) (dark green), of Aβ$_{4-16}$ (light blue) with 1 equivalent of Cu(I) (dark blue) and of Aβ$_{11-16}$ (light pink) with 1 equivalent of Cu(I) (dark pink) at pH 7.3 in phosphate buffer, His region (a) and Val12 region (b). The chemical shifts of His protons observed upon addition of Cu(I) are indicated with dotted lines.

**Affinity of Aβ$_{1/4//11-16}$ for Cu(I).** Cu(I) apparent binding affinity to Aβ$_{1/4//11-16}$ were determined by competition with the chromophoric $[Cu^{I}(Fz)_2]^{3-}$ (Fz = ferrozine = 5,6-diphenyl-3-(2-pyridyl)-1,2,4-triazine-4,4''-disulfonic acid) according to the model of Alies *et. al.* (Table 1 and Figure S4).[16b] This gives $K_a$ values of 1.9 ± 0.5 10$^{6}$ M$^{-1}$ and 3.7 ± 0.4 10$^{6}$ M$^{-1}$ for Cu$^{I}$(Aβ$_{11-16}$) and Cu$^{I}$(Aβ$_{4-16}$) respectively. Those values are of the same order of magnitude that the one reported in the literature by Alies *et al.* for the Cu$^{I}$(Aβ$_{1-16}$) complex (7.5 ± 1.0 10$^{6}$ M$^{-1}$) determined by the very same method. The two N-truncated peptides studied here are His–containing peptide sequences. It is then anticipated that Aβ$_{4/11-16}$ bind soft Cu(I) cation similarly to the Aβ$_{1-16}$ with two His in a linear geometry. The lower value found for Aβ$_{11-16}$ can be attributed to the lack of the third His (His6) in line with the weaker value reported for the mutated Aβ$_{1-16}$-H6A peptide.[16a, 16b] The two-fold weaker affinity for the 3-His containing Aβ$_{4-16}$ peptide may mirror second sphere effects due to modification of the N-terminal sequence, and is in line with modification of the Cu(I) affinity by acetylation of the terminal amine, previously reported.[16b]

We have described here the Cu(II) and Cu(I) coordination sites in the three peptides under study (Scheme 1) and also determine their Cu(I) affinity values (Table 1). From those values and the similarity of binding site, it is expected that the N-truncated peptides can compete with Aβ$_{1-16}$ peptide for Cu(I) coordination, but cannot remove Cu(I) from Cu$^{I}$Aβ$_{1-16}$. In contrast, the ATCUN peptides do remove Cu(II) from Cu$^{II}$Aβ$_{1-16}$.

**Reactive Oxygen Species (ROS) production.**

The intrinsic properties of Cu bound to the N-truncated Aβ to produce ROS in presence of ascorbate and $O_2$ were evaluated according to routine methods.[32] Briefly, in order to evaluate the ability of Cu to produce ROS when this latter is bound to the different peptides, an ascorbate consumption assay was performed in the presence of the different Aβ peptides, oxygen, and a slightly substoichiometric amount of Cu(II) (for details see ESI).[31, 33] The ascorbate concentration that fuels the reaction is followed by UV-vis at 265 nm.

**Starting from Cu(II)**. Compared to the Aβ$_{1-16}$ which produces a high level of ROS in these conditions, indicated by a quick and total consumption of the ascorbate in 2000 s (33 min), Aβ$_{4/11-16}$ prevent the formation of ROS (Figure S5). Between 2500 and 3000 s of the experiment, a rate constant for the ascorbate consumption around 0.04 ms$^{-1}$ is calculated (Figure 4a left). This basal consumption of ascorbate is attributed of the auto-oxidation of the ascorbate in our experimental conditions, indeed the same value is obtained with ascorbate only in the buffer (Figure S5). These results show the ability of both N-truncated peptides to chelate Cu(II) in the ATCUN motif, stabilizing the Cu(II) redox state under the Cu$^{II}$(Aβ$_{4/11-16}$)$_{ATCUN}$ complex and is in line with the low reduction potential of the Cu(II/I) couple observed by voltammetry. Those results are also in agreement with the reported lower level of hydroxyl radical produced with Cu$^{II}$(Aβ$_{4-16}$)$_{ATCUN}$ measured by APF (2-[6-(4'-amino)phenoxy-3H-xanthen-3-on-9-yl]benzoic acid) fluorescence in quite similar concentration conditions.[13a]

**Starting from Cu(II/I).** To go further and challenge the abilities of the Aβ$_{4/11-16}$ to stop ROS under more biologically relevant conditions, the ascorbate consumption assay was performed in

presence of Cu(I) and in presence of a mixture of Cu(I) and Cu(II). Such conditions could better mimic the extracellular brain environment, which is at the same time rich in ascorbate and dioxygen and where the predominant redox state of Cu is not determined.[34]

In order to obtain the Cu(II/I) mixture, Cu(II) was first reacted with ascorbate to generate Cu(I) by redox cycling and then the different Aβ peptide forms (*i. e.* $Aβ_{1-16}$ , $Aβ_{4-16}$ and $Aβ_{11-16}$) were added (Figure 3).

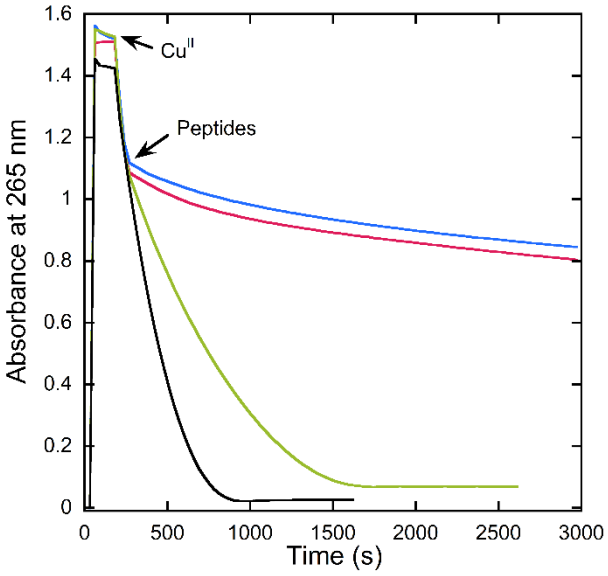


Figure 3: Kinetics of ascorbate consumption, followed by UV-visible spectroscopy at 265 nm. Asc + Cu(II) (black curve), Asc + Cu(II) + $Aβ_{1-16}$ (green curve), Asc + Cu(II) + $Aβ_{11-16}$ (pink curve), Asc + Cu(II) + $Aβ_{4-16}$ (blue curve). [$Aβ_{1/4/11-16}$] = 12 µM, [Cu(II)] = 10 µM, [Asc] = 100 µM, [HEPES] = 100 mM, pH 7.4.

Overall, the trend of the ascorbate consumption reflecting the ROS production is close to the one reported with Cu(II) only (Figure 3, Figure 4b left). Both N-truncated peptides are able to lower the consumption of ascorbate significantly compared to the non-truncated peptide $Aβ_{1-16}$. For $Aβ_{4/11-16}$, after 1500 s of reaction, the rate constant for the consumption of ascorbate are comparable with the one obtained with Cu(II) only, no matter the initial presence of Cu(I) (Figure 4d right). This observation indicates that at the end of the kinetic study the $Cu^{II}(Aβ_{4/11-16})_{ATCUN}$ complexes are the predominant species in solution. Hence we propose that the Cu(I) initially present has been oxidized in Cu(II), mainly generating the redox stable Cu(II) complexes as seen before.

However, the initial rates of the ascorbate consumption (between 260 and 900 s) are accentuated in presence of Cu(I) (Figure 4d left) compared to experiments done starting with Cu(II) only (Figure 4a). Quantitatively, in presence of Cu(I), the initial ascorbate consumption rate constants are four times higher (0.05 $ms^{-1}$ *vs* 0.21 $ms^{-1}$ for $Aβ_{4-16}$ and 0.07 $ms^{-1}$ *vs* 0.28 $ms^{-1}$ for $Aβ_{11-16}$). We hypothesized that a linear $Cu^{I}(Aβ_{4/11-16})$ complex is initially generated by the direct coordination of Cu(I) by the peptides and get oxidized by $O_2$ giving a Cu(II) species that may keep a linear coordination mode (Scheme 2). This new intermediate species named $Cu^{II}(Aβ_{4/11-16})_{L}$ (L for linear) can evolve in two different ways, (i) through a rearrangement to form the redox stable $Cu^{II}(Aβ_{4/11-16})_{ATCUN}$ (Scheme 2 black arrow) or (ii) can be reduced by ascorbate and thus produce ROS by redox cycling (Scheme 2 grey arrow). Therefore, the ROS production becomes dependent of the kinetic of the reduction of the transient $Cu^{II}(Aβ_{4/11-16})_{L}$ species *vs* its rearrangement into the $Cu^{II}(Aβ_{4/11-16})_{ATCUN}$ complex.


Scheme 2: Schematic representation of the formation of the transient $Cu^{II}(Aβ_{4/11-16})_{L}$ by oxidation of the $Cu^{I}(Aβ_{4/11-16})$ leading to either its re-organization into $Cu^{II}(Aβ_{4/11-16})_{ATCUN}$ (black arrow) or to its reduction (grey arrow).

In the presence of more peptide (2 equiv., see Figure S6), the rate of ascorbate consumption is slow down for all three peptides in line with previous report on $Aβ_{1-16}$,[17] and witness the decrease of the amount of free Cu.

**Starting from Cu(I) only**. In this experiment the Cu(I) is generated *in situ* directly in the sealed UV-vis cuvette by addition of ascorbate on a Cu(II) solution under anaerobic conditions. The different peptides are then added to the Cu(I)-asc solution to form the $Cu^{I}(Aβ_{1/4//11-16})$ species. The cuvette is finally opened at 1120 s and air is vigorously bubbled inside. The ascorbate consumption exhibits the same shape whether starting from Cu(I) or from the mixture of Cu(II/I) (Figure S7). The production of ROS is quicker at the beginning and stabilizes progressively to meet the level attributed to the auto-oxidation of the ascorbate, meaning a total arrest of the ROS production by the $Aβ_{4/11-16}$ peptides (Figure 4c left). Again we attribute this phenomenon to the oxidation of the $Cu^{I}(Aβ_{4/11-16})_{L}$ leading to a Cu(II) species which can be reduced by ascorbate or undergoes a rearrangement to form the redox inert $Cu^{II}(Aβ_{4/11-16})_{ATCUN}$ complex (Scheme 2).

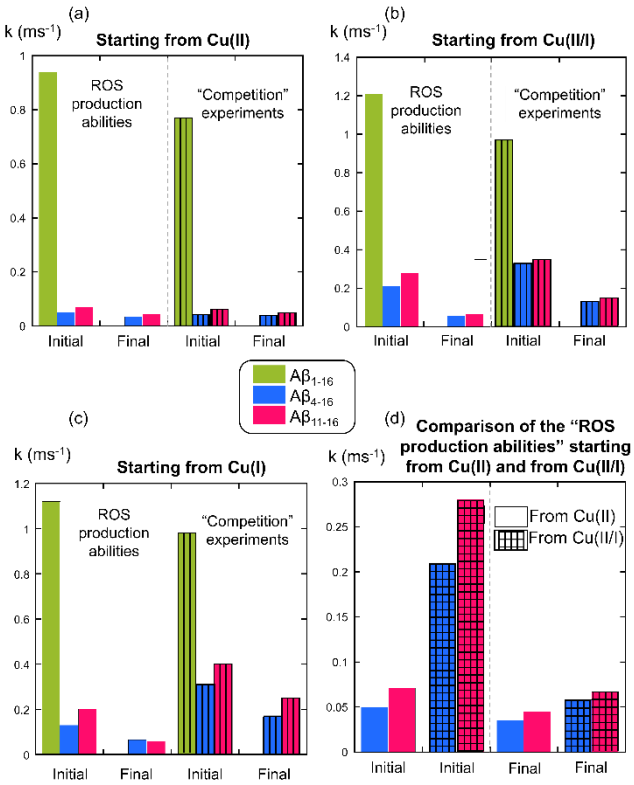


Figure 4: Rate constant of the ascorbate consumption of each experiments calculated at the beginning of the kinetics, during the first 5 minutes after the addition of the peptides (initial) and at the end during the 8 last minutes of the kinetics (final). Panel a : starting from Cu(II), panel b starting from Cu(II/I), panel c starting from Cu(I) and panel d comparison between panel a and panel b. Rate constants are calculated on at least three independent experiments with a good reproducibility for each condition, the mean values are plotted. On panel a, b and c the vertical striped bars represent experiments done with the N-truncated peptides used as a competitor compounds to extract Cu from Cu($A\beta_{1-16}$). On panel d the grid bars represent experiments starting from Cu(II/I). [$A\beta_{1/4/11-16}$] = 12 µM, [Cu(II)] = 10 µM, [Asc] = 100 µM, [HEPES] = 100 mM, pH 7.4.

### Ability of the N-truncated peptides to extract Cu(II) and Cu(I) from $A\beta_{1-16}$ peptide: Competition experiments.

**ROS from Cu(II).** As the N-truncated forms of the peptide ((*i. e.* $A\beta_{4-16}$ and $A\beta_{11-16}$) co-exist with non N-truncated forms (*i. e.* $A\beta_{1-16}$) in the brain,[3a-3c, 5] the effect on the ROS production of having in the experiments the two types of peptide (*i. e.* N-truncated and non-truncated) has been investigated. An ascorbate consumption assay was performed in presence of $O_2$ and an equimolar mixture of peptides being either $A\beta_{1-16}$ and $A\beta_{4-16}$ or $A\beta_{1-16}$ and $A\beta_{11-16}$, and a slightly substoechiometric amount of Cu(II) (Figure S8). In the presence of $A\beta_{4-16}$ or $A\beta_{11-16}$ and $Cu^{II}(A\beta_{1-16})$ the ascorbate consumption resemble to the one of the $Cu^{II}(A\beta_{4/11-16})$ (Figure 4a right). The formation of the thermodynamically stable $Cu^{II}(A\beta_{4/11-16})_{ATCUN}$ in line with the EPR data showing the removal of Cu(II) bound to $A\beta_{1-16}$ by the ATCUN-peptides prevents the production of ROS.

**Stopped-flow Cu(II) exchange kinetics.** The ability of the N-truncated peptides to extract Cu(II) from $Cu^{II}(A\beta_{1-16})$ has been investigated by stopped flow measurements.

The total extraction of the Cu(II) from the $A\beta_{1-16}$ is slow and takes about 60 s for both N-truncated peptides (Figure S9) with $A\beta_{4-16}$ faster than $A\beta_{11-16}$ in extracting Cu(II) ($t_{1/2}$ ± 15.5 s *vs* $t_{1/2}$ ± 10.8 s for $A\beta_{11-16}$ and $A\beta_{4-16}$ respectively).

**ROS from Cu(II/I)**. As previously described ROS production measurement was also conducted in the presence of Cu($A\beta_{1-16}$) in its two-redox forms. The experiment consisted to add ascorbate, to pre-form the $Cu^{II}(A\beta_{1-16})$ complex, and then to add the N-truncated peptides during ascorbate consumption (Figure 5, blue and pink curves)

The Cu induced ROS level increases in presence of $A\beta_{1-16}$ for both N-truncated peptides (compared Figure 3 *vs* Figure 5, and see figure 4b right). In other terms, the presence of $A\beta_{1-16}$ in the reaction medium slow down the formation of the redox stable $Cu^{II}(A\beta_{4/11-16})_{ATCUN}$ complex. As it was previously demonstrated (Table 1), the $A\beta_{1-16}$ cannot compete with the N-truncated peptides for the Cu(II) coordination, the difference in the ROS production is then assigned to the Cu(I) complexes formation, for which the $A\beta_{1-16}$ and the N-truncated peptides have the same affinity.

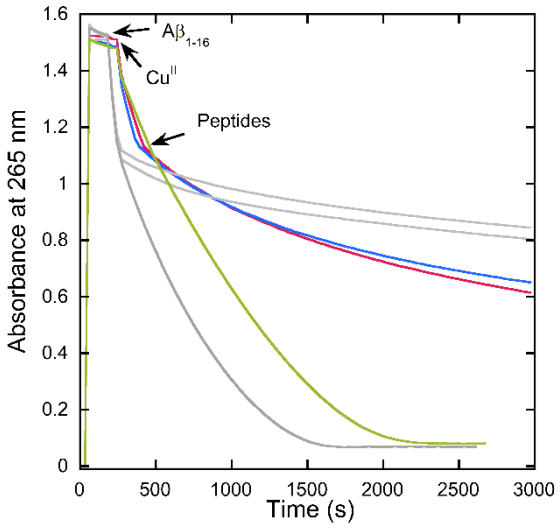


Figure 5 : Kinetics of ascorbate consumption, followed by UV-visible spectroscopy at 265 nm. Asc + $A\beta_{1-16}$ + Cu(II) + either $A\beta_{1-16}$ (green curve), or + $A\beta_{11-16}$ (pink curve), or + $A\beta_{4-16}$ (blue curve). The arrows indicate the order and time of the different addition into the UV-vis cuvette. [$A\beta_{1/4/11-16}$] = 12 µM or 24 µM (green curve), [Cu(II)] = 10 µM, [Asc] = 100 µM, [HEPES] = 100 mM, pH 7.4. The grey lines are the data presented in Figure 3 (Cu(II/I) + peptides), for comparison purpose.

The existence of an equilibrium between the different Cu(I) complexes (*i. e.* $Cu^{I}(A\beta_{4/11-16})$ and $Cu^{I}(A\beta_{1-16})$) would contribute to slow down the formation of the redox stable $Cu^{II}(A\beta_{4/11-16})_{ATCUN}$ complexes and maintain the $Cu^{I}(A\beta_{1-16})$ species in solution leading to a significant ROS production increase (Scheme 3b).

The ascorbate consumption experiment has also been performed by first adding the N-truncated peptides to the Cu(II/I) mixture allowing the formation of the $Cu^{II}(A\beta_{4/11-16})$ and $Cu^{I}(A\beta_{4/11-16})$ species and followed by the addition of the $A\beta_{1-16}$ at 25 s (before the full formation of the $Cu^{II}(A\beta_{4/11-16})_{ATCUN}$, Figure S10). Again, the ROS production increases in presence of $A\beta_{1-16}$ showing that the $Cu^{I}(A\beta_{1-16})$ complex, which produces ROS, can be quickly generated by exchange with the $Cu^{I}(A\beta_{4/11-16})$. The coordination and exchange processes are summarized in Scheme 3b.

**ROS from Cu(I).**

As expected, when the same competition experiment is done in presence of Cu(I) only the results obtained are similar (Figure 4c right and Figure S11).

**Proposed mechanisms.**

Based on the previously described studies, we here propose two mechanisms to explain ***(i)*** the ROS production of $Cu(A\beta_{4/11\text{-}16})$ (Scheme 3a) and ***(ii)*** the impact of $A\beta_{4/11\text{-}16}$ on the $Cu(A\beta_{1\text{-}16})$ ROS production (Scheme 3b).

***(i***) In presence of Cu(II), we observe the formation of complexes resistant to ascorbate reduction for the two N-truncated peptides (and thus there is no ROS produced) conversely to $Cu(A\beta_{1\text{-}16})$ (orange arrow in Scheme 3a). In presence of Cu(I) or Cu(II/I), the ROS production ability of the peptides differs. For the $Cu(A\beta_{1\text{-}16})$, its ability to catalyze the ROS formation has been widely studied before and is not dependent on the Cu redox starting state (See [[9]]). For the N-truncated peptides, we thus anticipate that a key step in the mechanism is the formation of a $Cu^{II}(A\beta_{4/11\text{-}16})_L$ intermediate species that can evolve either (i) back to the reduced counterpart (grey line in Scheme 2 and dotted grey line in Scheme 3a) or (ii) to the $Cu^{II}(A\beta_{4/11\text{-}16})_{ATCUN}$ site (black line in Scheme 2 and 3a). To validate such hypothesis, the Cu(II/I) ROS experiment were conducted with an higher ascorbate concentration, with the aim to favor the reduction of $Cu^{II}(A\beta_{4/11\text{-}16})_L$ (grey line in Scheme 2). It has to be noted that those conditions are probably closer to the AD brain environment were concentration up to the mM in ascorbate can be found.[35] At 500 µM of ascorbate $Cu(A\beta_{11\text{-}16})$ does produce ROS as much as the parent $Cu(A\beta_{1\text{-}16})$, while the ROS production level of $Cu(A\beta_{4\text{-}16})$ is similar to the one evaluated at 100 µM of ascorbate (Figure S12). There are two possible explanations: (a) the rate of the formation of the reduction-resistant $Cu^{II}(A\beta_{4/11\text{-}16})_{ATCUN}$ *versus* the rate of the reduction of the $Cu^{II}(A\beta_{4/11\text{-}16})_L$ is faster for $A\beta_{4\text{-}16}$ than $A\beta_{11\text{-}16}$ or (b) the amount of free $Cu^{I}$ contributing to the ROS produced is higher for $A\beta_{11\text{-}16}$ that has a weaker binding affinity (See Table 1). The identification of the Cu(II) binding site in the $Cu^{II}(A\beta_{4/11\text{-}16})_L$ species is beyond the scope of the present report based on *in-house* experience of similar studies on the $Cu(A\beta_{1\text{-}16})$ complex (see refs. [9a, 9e, 17, 36]). However we can propose a linearly bound Cu(II) species, where the Cu(II) might be linked by two His (reminiscent from $Cu^{I}$ site) or by one His and the N-terminal amine, based on recent articles aiming at deciphering the very first species appearing during the formation of $Cu^{II}(A\beta_{4\text{-}16})_{ATCUN}$ [21] and $Cu^{II}(GGH)_{ATCUN}$.[22]

(ii) In presence of $Cu^{II}(A\beta_{1\text{-}16})$, the time requested for getting the Cu(II) bound inside the N-truncated peptides is at least one order of magnitude longer than for Cu(II) (compare Figures S1 and S8) and there is no ROS produced provided that the mixture time between $Cu^{II}(A\beta_{1\text{-}16})$ and the $A\beta_{4/11\text{-}16}$ is long enough. In presence of $Cu^{II/I}(A\beta_{1\text{-}16})$, the main difference compared to Cu(II/I) is the almost equal distribution between $Cu^{I}(A\beta_{1\text{-}16})$ and $Cu^{I}(A\beta_{4\text{-}16})$ or $Cu^{I}(A\beta_{11\text{-}16})$ that decreases the amount of $Cu^{I}(A\beta_{4/11\text{-}16})$ present in the medium and thus the concentration of their oxidized counterparts. As a consequence, the formation of the $Cu^{II}(A\beta_{4/11\text{-}16})_{ATCUN}$ species is slowed down, allowing more ROS to be produced.

## Conclusion

In conclusion, in this work we have investigated the Cu(II) and Cu(I) binding properties of the N-truncated $A\beta_{11\text{-}16}$ and $A\beta_{4\text{-}16}$ peptide isoforms, and compared them to the $A\beta_{1\text{-}16}$. We show by EPR, electrochemistry and ascorbate consumption assays that $A\beta_{11\text{-}16}$ is able to form a redox inert Cu(II) complex and can extract Cu(II) from the $Cu^{II}(A\beta_{1\text{-}16})$ such as its analogue $A\beta_{4\text{-}16}$ that was previously studied. However, we demonstrate that the presence of the ATCUN motif into the N-truncated peptides that present high affinity constant for Cu(II) does not guaranty its redox inertness in presence of Cu(I). We then show that a key factor is the ratio between (i) the rate of reorganization of the intermediate $Cu^{II}(A\beta_{4/11\text{-}16})_L$ species into the $Cu^{II}(A\beta_{4/11\text{-}16})_{ATCUN}$ complex and (ii) the rate of its reduction to $Cu^{I}(A\beta_{4/11\text{-}16})$. Such ratio is different for both N-truncated peptides, with only the $A\beta_{4\text{-}16}$ being able to form the reduction-resistant ATCUN complex even at high ascorbate concentration. Hence, we can foresee that in biologically relevant conditions, the $A\beta_{4\text{-}16}$ doesn't participate in ROS formation, in contrast to the other two peptides.

A possible role of *in situ* generated ATCUN binding motif using peptide drug has been regarded as a possible therapeutic approach although requiring the modification of the sequence to render the peptide suitable for going through the blood brain barrier.[37] Along the same research line, other ATCUN peptides have also been studied.[38] Following a similar line of though, it could be anticipated that $A\beta_{4\text{-}16}$ could play a similar role, as a natural peptide drug, which would counterbalance the ROS produced by $Cu(A\beta_{1\text{-}16})$ by extracting Cu(II) and redox-silencing it. If one consider only the Cu(II) state, $A\beta_{4\text{-}16}$ is indeed able to extract it from $Cu(A\beta_{1\text{-}16})$ and further redox-silence it, thus preventing ROS formation by $Cu(A\beta_{1\text{-}16})$. However in presence of Cu(I), which is likely the most biologically relevant situation, the $A\beta_{4\text{-}16}$ is only able to lessen the ROS production of $Cu(A\beta_{1\text{-}16})$ but cannot fully preclude it as other synthetic molecules do.[39] This points out the importance of considering Cu(I) not only in the metal homeostasis in the synaptic cleft but also in the design of drug-candidates.

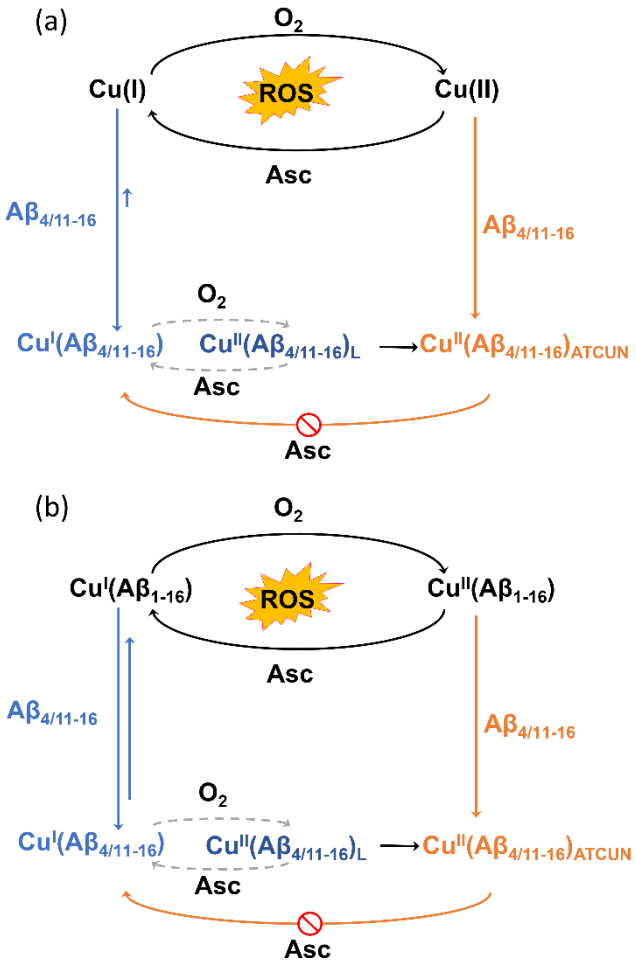


Scheme 3: Summary of Cu chelation and ROS production by the N-truncated peptides in absence (a) or in presence of $A\beta_{1-16}$ (b). The orange part represent the coordination of Cu(II) leading to the formation of an $Cu^{II}(A\beta_{4/11-16})_{ATCUN}$ complex inert toward ascorbate reduction. The blue part represent the Cu(I) coordination generating a Cu(I) complex which can be oxidized by $O_2$ to a transient species $Cu^{II}(A\beta_{4/11-16})_L$ where the Cu(II) is still bound linearly (dark blue). $Cu^{II}(A\beta_{4/11-16})_L$ can be reduce by ascorbate and generate ROS (dashed grey arrow) or can undergoes a rearrangement to form the redox inert $Cu^{II}(A\beta_{4/11-16})_{ATCUN}$ complex (full black arrow). In presence of $A\beta_{1-16}$ the Cu(I) is in equilibrium between the N-truncated forms and the $A\beta_{1-16}$ causing the production of more ROS.

## Experimental Section

**All chemicals** are from Sigma-Aldrich or TCI chemicals. The solutions were prepared in milliQ water (resistance: 18.2 MΩ.cm) except when notified. Cu(II) solution were prepared from a $CuSO_4.5H_2O$ salt and Cu(I) from a $Cu(CH_3CN)_4BF_4$ salt firstly dissolved in acetonitrile at a concentration around 1 mM, the exact concentration was determined by adding excess sodium bicinchoninic acid (BCA, 2-(4-carboxyquinolin-2-yl)quinoline-4-carboxylic acid) and measuring the absorbance of $Cu(BCA)_2^{3-}$ with an extinction coefficient of 7700 $M^{-1}$ $cm^{-1}$ at 562 nm. When notified, the Cu(I) was generated *in situ* by the reduction of Cu(II) with ascorbate for the ROS experiments or dithionite for the NMR experiments.

HEPES buffer (sodium salt of 2-[4-(2-hydroxyethyl)piperazin-1-yl]ethanesulfonic acid) was prepared at an initial concentration of 500 mM, pH 7.4.

Phosphate buffer, $K_2HPO_4$ and $KH_2PO_4$, were prepared at 500 mM, and they mixed until reaching a stock solution at 500 mM, pH 7.4.

Sodium ascorbate was prepared at 5 mM and freshly used.

Cu(peptides) complexes were *in situ* prepared by the mixing of the appropriate quantity of peptide stock solutions (about 1 mM) and $CuSO_4$ stock solution (about 1 mM) in a buffer (see figure captions for more details).

Ferrozine was prepared at 20 mM, pH 7.4, and titrated with the Cu(I) solution to determine the exact Fz concentration.

Peptides. $A\beta_{1-16}$, $A\beta_{4-16}$ and $A\beta_{11-16}$ (DAEFRHDSGYEVHHQK, FRHDSGYEVHHQK and EVHHQK respectively) were bought from Genecust. Stock solutions were prepared at around 10 mM and stored at 4°C. For Tyr containing peptide, concentration was determined by UV ($\varepsilon_{276-296}$= 1410 $cm^{-1}.M^{-1}$ at acidic pH). For the N-truncated peptides, the exact concentration was determined by a Cu(II) titration following the appearance of the d-d transition by UV-vis at the maximum absorption ($\lambda$ = 520 nm).

**UV-visible spectra** were recorded on a Hewlett Packard Agilent 8453 spectrophotometer at 25°C with an 800 rpm stirring.

**Affinity for Cu(I).** The apparent affinity constants at pH 7.4 of the Cu(I) complexes ($Cu^I(A\beta_{1-16})$, $Cu^I(A\beta_{4-16})$ and $Cu^I(A\beta_{11-16})$) were measured by UV-visible titrations in presence of ferrozine (Fz) as a competitor in a 1 cm sealed path length quartz cuvettes under argon, with an 800 rpm stirring. All the solution were prepared in Ar-degassed HEPES. The $Cu(Fz)_2^{3-}$ complex (55 µM) in HEPES (100 mM, pH 7.4) was firstly formed *in situ*, the different peptides were then added (ca. 100 µM per addition). The spectra were recorded and show the decrease of the 470 nm absorption band characteristic of the $Cu(Fz)_2^{3-}$ complex (with a molar extinction coefficient value ε = 4320 $M^{-1}$ $cm^{-1}$). The ($Cu^I(A\beta_{n-16})$ association constants were then determined using the binding constant of the $Cu(Fz)_2^{3-}$ (log $\beta_{12}$ = 11.6) described in the literature.

**Electron Paramagnetic Resonance.** Electron Paramagnetic Resonance (EPR) data were recorded using an Elexsys E 500 Bruker spectrometer, operating at a microwave frequency of approximately 9.5 GHz. Spectra were recorded using a microwave power of 2 mW across a sweep width of 150 mT (centered at 310 mT) with modulation amplitude of 0.5 mT. Experiments were carried out at 110 K using a liquid nitrogen cryostat.

EPR samples were prepared from stock solution of peptides diluted down to 0.2 mM in $H_2O$. 0.9 eq. of $^{65}Cu(II)$ was added from 78 mM $^{65}Cu(NO_3)_2$ stock solution home-made from a $^{65}Cu$ foil. If necessary, pH was adjusted to 7.4 with $H_2SO_4$ and NaOH solutions. Samples were frozen in quartz tube after addition of 10% glycerol as a cryoprotectant and stored in liquid nitrogen until used.

**Electrochemical experiments.** were performed in an argon-flushed cell. A three-electrode setup was used, and consists of a glassy carbon (3mm in diameter) disk as a working electrode, a platinum wire serves as auxiliary electrode and a Saturated Calomel Electrode as reference electrode directly dipped into the solution. Cyclic voltammograms were recorded with a Autolab PGSTAT302N potentiostat piloted by the EC-Lab software. The working electrode was carefully polished before each measurement on a red disk NAP with 1 µm AP-A suspension during at least one minute (Struers). Any support electrolyte was added because of the high concentration of phosphate buffer in the solution. The scanning speed was 0.1 $V.s^{-1}$. The samples were prepared from stock solutions of peptides and Cu(II) down to the desired concentration.

**Stopped-flow measurements**

Rapid-mixing UV-vis spectroscopy were carried out using a SFM-20 two syringes stopped-flow from Biologic combined with a diode array spectrometer composed of a TIDAS J&M MMS-UV/VIS 500-3 detector and a light source HAMAMATSU L7893 incorporating a deuterium and a tungsten lamps with optic fibers. Data acquisition, extraction and treatment were realized with the Bio-

Kine software. The syringes (Hamilton) are mounted on a rigid drive platform ensuring that the flow is stopped precisely and instantaneously. The contents of two syringes are rapidly mixed in the mixing chamber and the absorbance of the system recorded over time as full spectra at designated time delays. Typically, for the Cu(II) binding affinity one syringe was filled with a solution of peptide at 0.1 mM in HEPES buffer (200 mM, pH 7.4), the other one was filled with a solution of $CuSO_4$ in water at 0.08 mM. An equal quantity of the two solutions were mixed to reach a final concentration of $Cu^{II}$ of 416.5 µM and peptide of 500 µM in HEPES buffer (100 mM, pH 7.4). The $t_{1/2}$ was evaluated as the time requested to performed half of the reaction, *id est* the time requested to reach half of the maximum absorbance value at 520 nm.

**NMR**

The $^{1}H$ NMR experiments were recorded on a Bruker Avance NEO 600 spectrometer equipped with a 5mm broadband inverse triple-resonance probe $^{1}H$, BB ($^{31}P$-$^{103}Rh$)/$^{31}P$ with Z field gradients. The presaturation of the water signal was achieved with a zqpr sequence (Bruker). $^{1}H$ NMR experiments are performed at 298K. The peptides were dissolved in $D_2O$ and the concentration determined as previously described. All the manipulation described bellow were done under Ar, with Ar-degassed solutions. 2 equiv. (per Cu ion) of a 100 mM freshly prepared dithionite solution in $D_2O$ were added with a syringe to a CuSO4 solution in a 200 mM phosphate buffer in $D_2O$. 1 equiv. (per peptide) of the resulting Cu(I)-containing solution was immediately added to a degassed solution of peptide (Ar for 20 min). The resulting Cu(I) complex at 0.5 mM is then introduced with a syringe in an Ar-degassed NMR tube and sealed.

**ROS formation.** Ascorbate consumption was monitored by UV-Vis spectrophotometry. The decrease of the absorption band at $\lambda_{max}$ = 265 nm of the Asc (ε = 14 500 $M^{-1}.cm^{-1}$, corrected at 800 nm) was plotted as a function of time. The samples were prepared from stock solutions of peptides and Cu(II) diluted down to 12 and 10 µM respectively in HEPES (100 mM, pH 7.4) in a 1 cm or a 2 mm path length quartz cuvette. In the competition experiments, both peptides ($A\beta_{1-16}$ and $A\beta_{4/11-16}$) were at 12 µM. Ascorbate was added to obtain 100 µM or 500 µM as the final concentration. Final volume was adjusted with milliQ water to 2 mL.

## Acknowledgements

The authors thank the ERC aLzINK - Contract n° 638712 for financial support. CE thanks the PRESTIGE Programm for the grant n. PCOFUND-GA-2013-609102. The authors acknowledge Christian Bijani for the recording of the $^{1}H$ NMR spectra. Drs. Amandine Conte-Daban, Mireia Tomas I Giner and Laurent Sabater are gratefully acknowledge for their contributions and Dr. Karine Reybier for access to EPR facility.

**Keywords:** Amyloid peptides / Copper / ROS / Chelator / Bio-inorganic Chemistry

[1] J. Hardy, G. Higgins, *Science* **1992**, *256*, 184-185.

[2] a) E. Portelius, N. Bogdanovic, M. K. Gustavsson, I. Volkmann, G. Brinkmalm, H. Zetterberg, B. Winblad, K. Blennow, *Acta Neuropathol. (Berl).* **2010**, *120*, 185-193; b) C. L. Masters, G. Simms, N. A. Weinman, G. Multhaup, B. L. McDonald, K. Beyreuther, *Proc. Natl. Acad. Sci. U. S. A.* **1985**, *82*, 4245.

[3] a) K. Liu, I. Solano, D. Mann, C. Lemere, M. Mercken, J. Q. Trojanowski, V. M. Y. Lee, *Acta Neuropathol. (Berl).* **2006**, *112*, 163-174; b) V. Borghesani, B. Alies, C. Hureau, *Eur. J. Inorg. Chem.* **2018**, *2018*, 7-15; c) M. P. Kummer, M. T. Heneka, *Alzheimers Res Ther* **2014**, *6*, 28; d) V. Lanza, F. Bellia, E. Rizzarelli, *Coord. Chem. Rev.* **2018**, *369*, 1-14.

[4] S. Z. O. Wirths, S. Weggen (Ed.: T. Wisniewski), Alzheimer's Disease [Internet]. Brisbane (AU): Codon Publications, **2019**, pp. 107-122.

[5] J. Näslund, A. Schierhorn, U. Hellman, L. Lannfelt, A. D. Roses, L. O. Tjernberg, J. Silberring, S. E. Gandy, B. Winblad, P. Greengard, *Proc. Natl. Acad. Sci. U. S. A.* **1994**, *91*, 8378.

[6] Y. M. Kuo, T. A. Kokjohn, T. G. Beach, L. I. Sue, D. Brune, J. C. Lopez, W. M. Kalback, D. Abramowski, C. Sturchler-Pierrat, M. Staufenbiel, A. E. Roher, *J. Biol. Chem.* **2001**, *276*, 12991-12998.

[7] a) E. Stefaniak, W. Bal, *Inorg. Chem.* **2019**, *58*, 13561-13577; b) P. Gonzalez, K. Bossak, E. Stefaniak, C. Hureau, L. Raibaut, W. Bal, P. Faller, *Chem. Eur. J.* **2018**, *24*, 8029-8041; c) S. C. Drew, *Front. Neurosci.* **2017**, *11*, 317.

[8] C. Hureau, in *Encyclopedia of Inorganic and Bioinorganic Chemistry* (Ed.: R. A. Scott), **2019**, pp. 1-14.

[9] a) V. Balland, C. Hureau, J.-M. Savéant, *Proc. Natl. Acad. Sci. U. S. A.* **2010**, *107*, 17113-17118; b) C. Hureau, V. Balland, Y. Coppel, P. L. Solari, E. Fonda, P. Faller, *J. Biol. Inorg. Chem.* **2009**, *14*, 995-1000; c) C. Hureau, P. Faller, *Biochimie* **2009**, *91*, 1212-1217; d) L. G. Trujano-Ortiz, F. J. González, L. Quintanar, *Inorg. Chem.* **2015**, *54*, 4-6; e) C. Cheignon, M. Jones, E. Atrián-Blasco, I. Kieffer, P. Faller, F. Collin, C. Hureau, *Chem. Sci.* **2017**, *8*, 5107-5118.

[10] C. Hureau, *Coord. Chem. Rev.* **2012**, *256*, 2164-2174.

[11] a) E. Atrián-Blasco, P. Gonzalez, A. Santoro, B. Alies, P. Faller, C. Hureau, *Coord. Chem. Rev.* **2018**, *371*, 38-55; b) S. C. Drew, K. J. Barnham, *Acc. Chem. Res.* **2011**, *44*, 1146-1155; c) C. Hureau, P. Dorlet, *Coord. Chem. Rev.* **2012**, *256*, 2175-2187.

[12] a) B. Alies, E. Renaglia, M. Rózga, W. Bal, P. Faller, C. Hureau, *Anal. Chem.* **2013**, *85*, 1501-1508; b) A. Conte-Daban, V. Borghesani, S. Sayen, E. Guillon, Y. Journaux, G. Gontard, L. Lisnard, C. Hureau, *Anal. Chem.* **2017**, *89*, 2155-2162.

[13] a) M. Mital, N. E. Wezynfeld, T. Frączyk, M. Z. Wiloch, U. E. Wawrzyniak, A. Bonna, C. Tumpach, K. J. Barnham, C. L. Haigh, W. Bal, S. C. Drew, *Angew. Chem. Int. Ed.* **2015**, *54*, 10460-10464; b) J. D. Barritt, J. H. Viles, *J. Biol. Chem.* **2015**, *290*, 27791-27802.

[14] T. Kowalik-Jankowska, M. Ruta-Dolejsz, K. Wiśniewska, L. Łankiewicz, H. Kozłowski, *J. Chem. Soc., Dalton Trans.* **2000**, 4511-4519.

[15] a) G. De Gregorio, F. Biasotto, A. Hecel, M. Luczkowski, H. Kozlowski, D. Valensin, *J. Inorg. Biochem.* **2019**, *195*, 31-38; b) J. Shearer, V. A. Szalai, *J. Am. Chem. Soc.* **2008**, *130*, 17826-17835.

[16] a) T. R. Young, A. Kirchner, A. G. Wedd, Z. Xiao, *Metallomics* **2014**, *6*, 505-517; b) B. Alies, B. Badei, P. Faller, C. Hureau, *Chem. Eur. J.* **2012**, *18*, 1161-1167; c) Z. Xiao, L. Gottschlich, R. van der Meulen, S. R. Udagedara, A. G. Wedd, *Metallomics* **2013**, *5*, 501-513.

[17] E. Atrián-Blasco, M. del Barrio, P. Faller, C. Hureau, *Anal. Chem.* **2018**, *90*, 5909-5915.

[18] F. Arrigoni, T. Prosdocimi, L. Mollica, L. De Gioia, G. Zampella, L. Bertini, *Metallomics* **2018**, *10*, 1618-1630.

[19] a) M. J. Pushie, E. Stefaniak, M. R. Sendzik, D. Sokaras, T. Kroll, K. L. Haas, *Inorg. Chem.* **2019**, *58*, 15138-15154; b) V. A. Streltsov, R. S. K. Ekanayake, S. C. Drew, C. T. Chantler, S. P. Best, *Inorg. Chem.* **2018**, *57*, 11422-11435.

[20] N. E. Wezynfeld, E. Stefaniak, K. Stachucy, A. Drozd, D. Płonka, S. C. Drew, A. Krężel, W. Bal, *Angew. Chem. Int. Ed.* **2016**, *55*, 8235-8238.

[21] X. Teng, E. Stefaniak, P. Girvan, R. Kotuniak, D. Płonka, W. Bal, L. Ying, *Metallomics* **2020**, *12*, 470-473.

[22] R. Kotuniak, M. J. F. Strampraad, K. Bossak-Ahmad, U. E. Wawrzyniak, I. Ufnalska, P.-L. Hagedoorn, W. Bal, *Angew. Chem. Int. Ed.* **2020**, *59*, 11234-11239.

[23] a) S. E. Conklin, E. C. Bridgman, Q. Su, P. Riggs-Gelasco, K. L. Haas, K. J. Franz, *Biochemistry* **2017**, *56*, 4244-4255; b) K. L. Haas, A. B. Putterman, D. R. White, D. J. Thiele, K. J. Franz, *J. Am. Chem. Soc.* **2011**, *133*, 4427-4437.

[24] P. Gonzalez, K. Bossak-Ahmad, B. Vileno, N. E. Wezynfeld, Y. El Khoury, P. Hellwig, C. Hureau, W. Bal, P. Faller, *Chem. Commun.* **2019**, *55*, 8110-8113.

[25] J. W. Karr, H. Akintoye, L. J. Kaupp, V. A. Szalai, *Biochemistry* **2005**, *44*, 5478-5487.

[26] T. A. Enache, A. M. Oliveira-Brett, *J. Electroanal. Chem.* **2011**, *655*, 9-16.
[27] M. Z. Wiloch, I. Ufnalska, A. Bonna, W. Bal, W. Wróblewski, U. E. Wawrzyniak, *J. Electrochem. Soc.* **2017**, *164*, G77-G81.
[28] a) P. Gonzalez, B. Vileno, K. Bossak, Y. El Khoury, P. Hellwig, W. Bal, C. Hureau, P. Faller, *Inorg. Chem.* **2017**, *56*, 14870-14879; b) C. Hureau, H. Eury, R. Guillot, C. Bijani, S. Sayen, P.-L. Solari, E. Guillon, P. Faller, P. Dorlet, *Chemistry – A European Journal* **2011**, *17*, 10151-10160.
[29] N. E. Wezynfeld, A. Tobolska, M. Mital, U. E. Wawrzyniak, M. Z. Wiloch, D. Płonka, K. Bossak-Ahmad, W. Wróblewski, W. Bal, *Inorg. Chem.* **2020**, *59*, 14000-14011.
[30] a) B. Alies, C. Bijani, S. Sayen, E. Guillon, P. Faller, C. Hureau, *Inorg. Chem.* **2012**, *51*, 12988-13000; b) H. Eury, C. Bijani, P. Faller, C. Hureau, *Angew. Chem. Int. Ed.* **2011**, *50*, 901-905; c) A. Jancsó, K. Selmeczi, P. Gizzi, N. V. Nagy, T. Gajda, B. Henry, *J. Inorg. Biochem.* **2011**, *105*, 92-101; d) C. Livera, L. D. Pettit, M. Bataille, J. Krembel, W. Bal, H. Kozlowski, *J. Chem. Soc., Dalton Trans.* **1988**, 1357-1360.
[31] A. Conte-Daban, B. Boff, A. Candido, C. Montes Aparicio, C. Gateau, C. Lebrun, G. Cerchiaro, I. Kieffer, S. Sayen, E. Guillon, P. Delangle, C. Hureau, *Chem. Eur. J.* **2017**, *23*, 17078-17088.
[32] a) S. Chassaing, F. Collin, P. Dorlet, J. Gout, C. Hureau, P. Faller, *Curr. Top. Med. Chem.* **2012**, *12*, 2573-2595; b) B. Alies, I. Sasaki, O. Proux, S. Sayen, E. Guillon, P. Faller, C. Hureau, *Chem. Commun.* **2013**, *49*, 1214-1216.
[33] A. Conte-Daban, A. Day, P. Faller, C. Hureau, *Dalton Trans.* **2016**, *45*, 15671-15678.
[34] a) R. Figueroa-Méndez, S. Rivas-Arancibia, *Front. Physiol.* **2015**, *6*; b) A. Carreau, B. E. Hafny-Rahbi, A. Matejuk, C. Grillon, C. Kieda, *J. Cell. Mol. Med.* **2011**, *15*, 1239-1253.
[35] F. E. Harrison, J. M. May, *Free Radic. Biol. Med.* **2009**, *46*, 719-730.
[36] a) C. Cheignon, P. Faller, D. Testemale, C. Hureau, F. Collin, *Metallomics* **2016**, *8*, 1081-1089; b) L.-E. Cassagnes, V. Hervé, F. Nepveu, C. Hureau, P. Faller, F. Collin, *Angew. Chem. Int. Ed.* **2013**, *52*, 11110-11113.
[37] D. S. Folk, K. J. Franz, *J. Am. Chem. Soc.* **2010**, *132*, 4994-4995.
[38] a) A. B. Caballero, L. Terol-Ordaz, A. Espargaró, G. Vázquez, E. Nicolás, R. Sabaté, P. Gamez, *Chem. Eur. J.* **2016**, *22*, 7268-7280; b) X. Hu, Q. Zhang, W. Wang, Z. Yuan, X. Zhu, B. Chen, X. Chen, *ACS Chem. Neurosci.* **2016**, *7*, 1255-1263.
[39] C. Esmieu, D. Guettas, A. Conte-Daban, L. Sabater, P. Faller, C. Hureau, *Inorg. Chem.* **2019**, *58*, 13509-13527.
…

**Entry for the Table of Contents** (Please choose one layout)

---

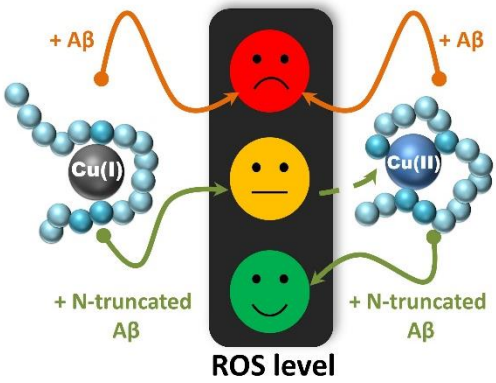


The ability of N-truncated amyloid-β peptides to contribute and/or prevent the production of deleterious reactive oxygen species by Cu or Cu(amyloid-β) is under focus and the key role of copper(I) evidenced